ChemistryOpen

Research Article
doi.org/10.1002/open.202200063

Chemistry Europe
European Chemical
Societies Publishing

www.chemistryopen.org

Cluster Compounds with Oxidised, Hexanuclear [Nb$_6$Cl$^i_{12}$I$^a_6$]$^{n-}$ Anions ($n = 2$ or 3)

Florian Schröder[a] and Martin Köckerling*[a, b]

Four mixed-halide cluster salts with chloride-iodide-supported octahedral Nb$_6$ metal atoms cores were prepared and investigated. The cluster anions have the formula [Nb$_6$Cl$^i_{12}$I$^a_6$]$^{n-}$ with Cl occupying the inner ligand sites and I the outer one. They are one- or two-electron-oxidized ($n = 2$ or 3) with respect to the starting material cluster. (Ph$_4$P)$^+$ and (PPN)$^+$ function as counter cations. The X-ray structures reveal a mixed occupation of the outer sites for only one compound, (PPN)$_3$[Nb$_6$Cl$^i_{12}$I$^a_{5.047(9)}$Cl$^a_{0.953}$]. All four compounds are obtained in high yield. If in the chemical reactions a mixture of acetic anhydride, CH$_2$Cl$_2$, and trimethylsilyl iodide is used, the resulting acidic conditions lead to form the two-electron-oxidised species ($n = 2$) with 14 cluster-based electrons (CBEs). If only acetic anhydride is used, the 15 CBE species ($n = 3$) is obtained in high yield. Interesting intermolecular bonding is found in (Ph$_4$P)$_2$[Nb$_6$Cl$^i_{12}$I$^a_6$]·4CH$_2$Cl$_2$ with I···I halogen bonding and π-π bonding interactions between the phenyl rings of the cations in (PPN)$_3$[Nb$_6$Cl$^i_{12}$I$^a_{5.047(9)}$Cl$^a_{0.953}$]. The solubility of (Ph$_4$P)$_2$[Nb$_6$Cl$^i_{12}$I$^a_6$]·4CH$_2$Cl$_2$ has been determined qualitatively in a variety of solvents, and good solubility in the aprotic solvents CH$_3$CN, THF and CH$_2$Cl$_2$ has been found.

Introduction

Reduced halides and oxides of electron-poor transition metals often contain polyhedral arrangements of metal atoms with strong metal-metal bonds. Such cluster complexes are an intensively investigated field of research in solid-state and solution chemistry for decades.[1–21] The large group of cluster compounds with octahedral metal atom polyhedra of the IVB and VB group metals are particularly in focus.[22–26] The M_6 octahedra are surrounded by a ligand sphere of either eight (for $M = $ Nb and $X = $ I; [M_6X_8] cluster type) or twelve "inner" ligands X^i, ($X^i = $ Cl or Br; [M_6X_{12}] type). In the [M_6X_8] cluster type, the X^i ligands bridge the faces of the M_6 octahedron and in the [M_6X_{12}] type the edges.[27–28] The cluster units of both types contain, on the octahedral *exo*-sites, six additional X^a ligands. The [$M_6X^i_8X^a_6$] and [$M_6X^i_{12}X^a_6$] cluster units have been shown to exist in three different oxidation states. In the [M_6X_{12}] type, these go along with 16, 15, or 14 (cluster-based) electrons (CBEs) located in the highest occupied orbitals which are, to a large extent, metal-centred. The HOMO of non-oxidized cluster cores with 16 CBEs has a$_{2u}$ symmetry and is metal-metal bonding and metal-X^i

antibonding in character. The removal of electrons from this orbital results in cluster units with 15 or 14 CBEs.[29–31]

Surveying the literature shows that, so far, the Nb$_6$ and Ta$_6$ iodides are much less investigated than the chlorides and bromides. This is despite the fact that the few known niobium cluster iodides, [Nb$_6$I$_{11}$], Cs[Nb$_6$I$_{11}$], [Nb$_6$I$_9$S], and their hydrides as well as [Nb$_6$I$_8$(NH$_2$R)$_6$] ($R = $ CH$_3$, C$_3$H$_7$), [Nb$_6$I$_8$Py$_6$] and [Nb$_6$I$_8$Py$_6$]I·9Py (py = pyridine) are rare examples of [M_6X_8] type group VB cluster compounds. Furthermore, some of them exhibit very interesting magnetic properties.[32–40] In contrast to niobium, the homologous element tantalum forms iodide-supported cluster units of the [M_6X_{12}] type.[41]

In this paper, we report about oxidised mixed chloride-iodide-supported hexanuclear niobium cluster compounds with 14 or 15 CBEs. These are (Ph$_4$P)$_3$[Nb$_6$Cl$_{12}$I$_6$] (**1**), (Ph$_4$P)$_2$[Nb$_6$Cl$_{12}$I$_6$]·4CH$_2$Cl$_2$ (**2**), (PPN)$_3$[Nb$_6$Cl$^i_{12}$I$^a_{5.047(9)}$Cl$^a_{0.953}$] (**3**) and (PPN)$_2$[Nb$_6$Cl$_{12}$I$_6$]·2CH$_2$Cl$_2$ (**4**), which were synthesized and characterized by X-ray diffraction analysis, IR-, NMR-, and X-ray photoelectron spectroscopy, as well as by elemental analyses.

Results and Discussion

Synthesis

The stepwise substitution of halogenido ligands in octahedral M_6 cluster complexes by other halides (mixed halide cluster systems) allows for a more or less stepwise modification of chemical properties, for example of UV-Vis absorption properties (colour), redox potentials or solubilities. Because of the presence of two distinct different coordination spheres, inner (i) and outer (a) in [$M_6X^i_{12}X^a_6$] type cluster compounds, we started to search for preparative procedures for mixed chloride-iodide-supported cluster complexes with only one halide type on each of the two different coordination site types, that is, cluster

[a] M.Sc. F. Schröder, Prof. Dr. M. Köckerling
Universität Rostock
Institut für Chemie
Anorganische Festkörperchemie
Albert-Einstein-Str. 3a
18059 Rostock (Germany)
E-mail: Martin.Koeckerling@uni-rostock.de
[b] Prof. Dr. M. Köckerling
Universität Rostock
Department Life, Light and Matter
18051 Rostock (Germany)

ChemistryOpen

Research Article
doi.org/10.1002/open.202200063

Chemistry Europe
European Chemical
Societies Publishing

anions of the type $[Nb_6Cl^i_{12}I^a_6]$. Preliminary preparative investigations starting from $[Nb_6Cl^i_{12}(H_2O)^a_4Cl^a_2]\cdot 4H_2O$ and a large excess of $(R_4N)I$ ($R = C_2H_5$ or nC_4H_9) gave Nb_6 cluster complex units with mixed Cl an I occupation on both the X^i and X^a sites. Therefore, we changed the starting material to $[Nb_6Cl^i_{12}I^a_2(H_2O)^a_4]\cdot 4H_2O$, which has already two of the outer coordination sites occupied by iodide ligands. Tetraphenyl phosphonium iodide, $(Ph_4P)I$, and μ-nitrido-bis(triphenylphosphane) iodide, $(PPN)I$, were used as sources for the remaining iodide anions and counter cations. The substitution of the water ligands in the starting material is accelerated by the addition of acetic anhydride. This leads to acidic reactions conditions, in which the 16 CBE-containing cluster core is oxidised by one electron, if the reaction is done using Ac_2O only. If a mixture of Ac_2O, CH_2Cl_2, and (TMS)I is used, a two-electron oxidation is achieved, leading to the 14 CBE-containing $[Nb_6Cl^i_{12}I^a_6]^{2-}$ units. This successful concept of treating $[Nb_6Cl^i_{12}X^a_2(H_2O)^a_4]\cdot 4H_2O$ ($X = Cl$ or I) with a water scavenger acting as reactant, solvent and oxidiser, and supplying further ligands has been introduced before.[42–50] All four investigated compounds are obtained in high yield. The experimental conditions for the synthesis of **1** to **4** are summarized in Scheme 1.

In the cases of **1**, **2**, and **4**, a complete occupation of the X^a site with iodide is achieved without any mixed-halide occupation. In the case of the $(PPN)^+$-based cluster compound **3**, the structure analysis shows some mixed occupation of the outer sites to a minor extent (see below).
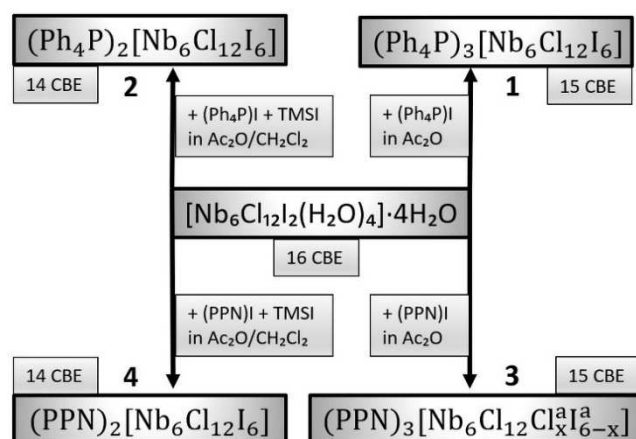
Structures

All four new cluster compounds described in this paper consist of octahedral Nb_6 cluster cores with 12 Cl atoms μ$_2$-bonded on the inner coordination sites and I atoms on the outer ones. The charges of the discrete $[Nb_6Cl^i_{12}I^a_6]^{n-}$ ($n = 2$ in **2** and **4**, $n = 3$ in **1** and **3**) are compensated by either $(Ph_4P)^+$ (**1** and **2**) or $(PPN)^+$ (μ-nitrido-bis(triphenylphosphane) **3** and **4**) cations. The ratio of

the number of cations to cluster anions allows for the assignment of $n = 2$ for **2** and **4** and $n = 3$ for **1** and **3**.
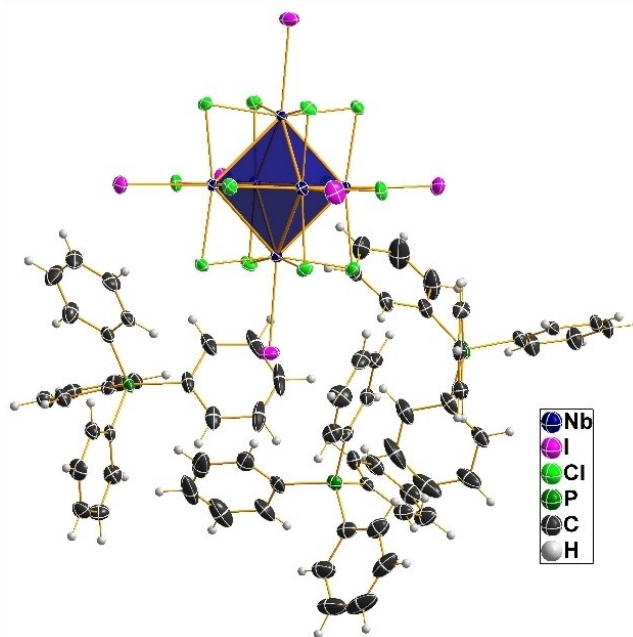
All cluster units carry only Cl atoms on the inner halide sites. Whereas in the cluster units of **1**, **2**, and **4** the outer coordination sites are only occupied by I, the crystal structure analysis reveals a mixed Cl/I occupation with the finally refined composition $(PPN)_3[Nb_6Cl^i_{12}I^a_{5.047(9)}Cl^a_{0.953}]$ for **3**. In the crystal structure refinement, the sum of the occupational factors for each outer halide site was fixed to full occupation. The phase width for $(PPN)_3[Nb_6Cl^i_{12}I^a_{6-x}Cl^a_x]$ is expected to be $x \leq 6$. Crystals of **2** and **4** contain further co-crystallized dichloromethane molecules.

Figures 1–4 show the cation-cluster anion pairs in the structures of the four compounds. Table 1 details the crystallographic and refinement data. Ranges and average values of selected interatomic distances are compiled in Table 2.
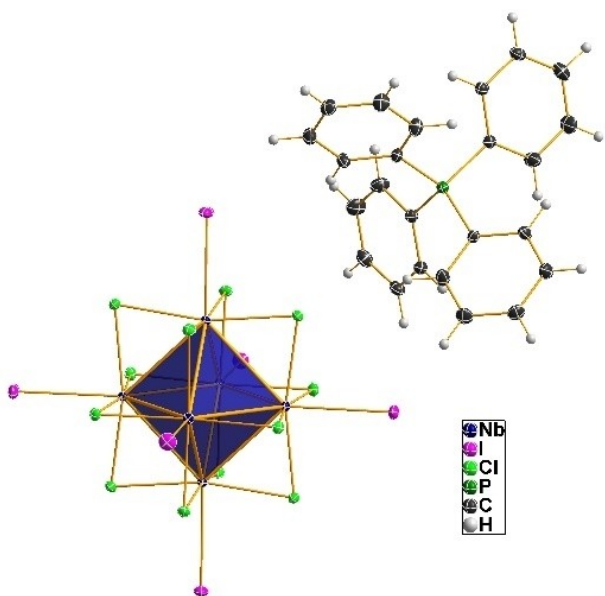
The conclusion of the charges of 2-, and 3-, respectively, on the cluster anions from the cation-anion ratio of the X-ray structure analysis and thereby the corresponding number of CBEs of 14 and 15 is in line with the observed Nb–Nb and Nb–Cl^i distances. Such distances have been shown to depend significantly on the number of CBEs present as well as on the size of the coordinated ligand atoms (matrix effect). Because of the metal-metal bonding and metal-X^i antibonding character of the a_{2u} HOMO of 16 CBE-cluster units, the M–M bond lengths increase and the M–X^i distances decrease on oxidation.[29–30,51] The average Nb–Nb distances in the 15 CBE cluster anions are determined at 2.9831 Å (**1**) and 2.9798 Å (**3**). They are found in the range of the values of other 15 CBE $[Nb_6Cl^i_{12}]$ cluster units. In compounds with the $[Nb_6Cl_{18}]^{3-}$ cluster anion, the range is from 3.003 Å in $[(18\text{-}cr\text{-}6)(H_5O_2)]_3[Nb_6Cl_{18}]$ to 2.956 Å in Lu-$[Nb_6Cl_{18}]$.[52–58] An even smaller value of 2.9506 Å is found in

$(Ph_4P)_2[Nb_6Cl_{12}I_6]$
14 CBE **2**

$(Ph_4P)_3[Nb_6Cl_{12}I_6]$
1 15 CBE

+ $(Ph_4P)I$ + TMSI
in Ac_2O/CH_2Cl_2

+ $(Ph_4P)I$
in Ac_2O

$[Nb_6Cl_{12}I_2(H_2O)_4]\cdot 4H_2O$
16 CBE

+ $(PPN)I$ + TMSI
in Ac_2O/CH_2Cl_2

+ $(PPN)I$
in Ac_2O

14 CBE **4**
$(PPN)_2[Nb_6Cl_{12}I_6]$

3 15 CBE
$(PPN)_3[Nb_6Cl_{12}Cl^a_xI^a_{6-x}]$

Scheme 1. Reaction scheme for the synthesis of **1–4**.

Figure 1. Structure of the cluster anion and $(Ph_4P)^+$ cations in crystals of $(Ph_4P)_3[Nb_6Cl_{12}I_6]$ (**1**). Displacement ellipsoids are shown at the 50% probability level and the Nb_6 core is shown in a polyhedral representation.

ChemistryOpen

Research Article
doi.org/10.1002/open.202200063

**Chemistry
Europe**
European Chemical
Societies Publishing

Figure 2. Structure of the cluster anion and the $(Ph_4P)^+$ cation in crystals of $(Ph_4P)_2[Nb_6Cl_{12}I_6] \cdot 4CH_2Cl_2$ (**2**). Displacement ellipsoids are shown at the 50% probability level. The dichloromethane molecules have been omitted for clarity.
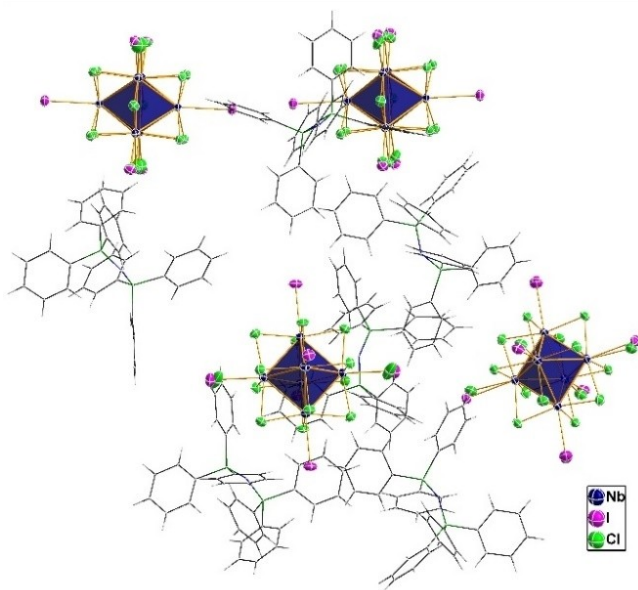
Figure 3. Structure of the four symmetry independent cluster anions and the $(PPN)^+$ cations in crystals of $(PPN)_3[Nb_6Cl^i_{12}I^a_{5.05}Cl^a_{0.95}]$ (**3**). Displacement ellipsoids are shown at the 50% probability level. The cations are shown in a wire-stick representation.

$[Nb_6Cl_{12}(PrCN)_6][SbCl_3]$ which can be explained by the much less pronounced matrix-effect of the *exo*-N-bonded propionitrile compared to the chloride ligands.[22,59–60]

The average $Nb–Cl^i$ distances in **1** and **3** with values of 2.435 Å and 2.433 Å compare well with that found for example in $Lu[Nb_6Cl_{18}]$ (2.432 Å).[53] As expected, they are shorter than those found in 16 CBE cluster units, for example in $K_4[Nb_6Cl_{18}]$
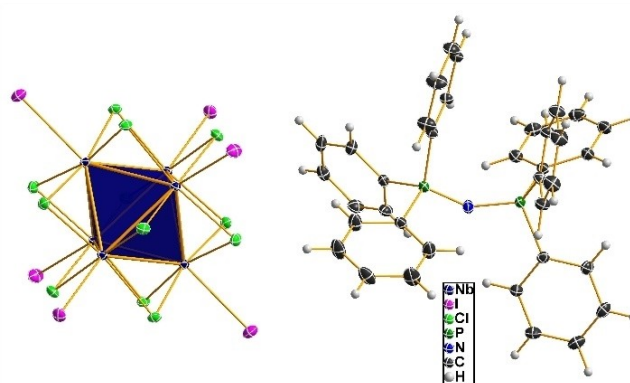
Figure 4. Structure of the cluster anion and $(PPN)^+$ cation in crystals of $(PPN)_2[Nb_6Cl_{12}I_6] \cdot 2CH_2Cl_2$ (**4**). Displacement ellipsoids are shown at the 50% probability level and the co-crystallised methylene chloride molecules are omitted for clarity

which has an average $Nb–Cl^i$ distance of 2.49 Å.[61–62] All four title compounds have I atoms bonded apically to the Nb_6 octahedron, with **3** having some admixture of Cl atoms, see above. In the 15 CBE cluster units of **1** and **3**, significantly longer distances to the Nb atoms (in average 2.9239 Å and 2.932 Å) are observed compared to those of the 14 CBE units in **2** and **4** (2.8708 Å and 2.8773 Å).

A further comparison of such distances with other cluster compounds is difficult, because in all the few so far known iodide supported Nb_6 cluster compounds the I atoms are involved in inter-cluster bridging. Therefore, the distances are not comparable to those of the terminal bonded I^a atoms of the title compounds. The trend of increasing Nb–Nb and decreasing $Nb–Cl^i$ and $Nb–I^a$ distances continues on going from the 15 CBE cluster units to the 14 CBE units in **2** and **4**, see Table 2.

As in most cases of Nb_6 cluster salts, the ions are arranged in some sort of (dense) packing. Potentially, voids between the ions are filled with co-crystallized solvent molecules. Exemplarily for the title compounds, the ion packing in crystals of **3** is shown in Figure 5.

Intermolecular interactions besides van-der-Waals and coulombic forces influence the arrangement of the structural units in all structures discussed in this paper. In crystals of **1** weak C–H···I hydrogen bonds exist with the shortest D···A distance of 3.819(6) Å. In **2**, shorter hydrogen bonds exist between the I^a atoms and the H atoms of the co-crystalline dichloromethane molecules with D···A distances in the range of 3.761(2) Å to 3.959(2) Å.

The cluster units in **2** are arranged in chains along the crystallographic *c* direction with intermolecular $I^a···I^a$ distances of 4.0340(5) Å and a $Nb–I^a···I^a$ angle of 180°. This angle and the distance being close to the van-der-Waals distance of two iodine atoms indicate some attractive halogen bonding.[63–66] As shown in Figure 6, some I···H hydrogen bonding is present in addition to the halogen bonding.

In crystals of **3**, phenyl rings of neighbouring $(PPN)^+$ cations are arranged parallelly with a centre···centre distance of 4.056 Å, indicating π-π interactions, see Figure 7.[67–68]

Table 1. Crystal data and numbers pertinent to data collection and structure refinement for the compounds **1–4**.

Compound	1	2	3	4
Empirical formula	$C_{72}H_{60}Cl_{12}I_6Nb_6P_3$	$C_{52}H_{48}Cl_{20}I_6Nb_6P_2$	$C_{108}H_{90}Cl_{12.953(9)}I_{5.047}Nb_6P_6N_3$	$C_{74}H_{64}Cl_{16}I_6N_2Nb_6P_4$
Fw/g·mol^{-1}	2762.37	2762.70	3271.66	2991.21
Crystal System	monoclinic	tetragonal	triclinic	triclinic
Space group	$P2_1/n$	$P4/n$	$P\bar{1}$	$P\bar{1}$
a/Å	14.224(1)	16.717(1)	14.692(2)	9.8807(7)
b/Å	16.392(1)	16.717(1)	28.667(4)	15.463(1)
c/Å	37.482(3)	14.058(2)	30.101(4)	16.110(1)
α/°	90	90	67.144(2)	106.555(2)
β/°	97.410(3)	90	82.103(2)	95.434(2)
γ/°	90	90	87.541(2)	95.955(2)
V/Å^3	8667(1)	3928.8(8)	11571(3)	2326.5(3)
Z	4	2	4	1
T/K	123(2)	123(2)	123(2)	123(2)
μ/mm^{-1} (MoKα)	3.326	3.908	2.318	3.233
2θ(max.)/°	53.154	70.122	53.426	70.224
No. indep. Refl., R_{int}	18046, 6.81	8688, 4.04	48518, 6.77	20575, 4.91
No. of parameters	892	199	2597	487
GOOF on F^2	1.032	1.072	1.043	1.072
R1 [I $>$ 2σ(I)][a]	3.89	1.90	3.95	2.68
wR2 [I $>$ 2σ(I)][b]	7.29	3.69	7.89	5.71
R1 (all data)[a]	6.65	3.16	6.25	3.77
wR2 (all data)[b]	8.25	4.11	8.94	6.32
A, B[b]	0.0216, 42.4467	0.0132, 4.6029	0.0290, 33.2619	0.0175, 3.6423

a) $R1 = \dfrac{\sum ||F_0| - |F_c||}{\sum |F_0|}$; $wR2 = \sqrt{\dfrac{\sum w(F_0^2 - F_c^2)^2}{\sum w(F_0^2)^2}}$; b) $w = \dfrac{1}{\sigma^2(F_0^2) + (AP)^2 + BP}$; $P = \dfrac{F_0^2 + 2F_c^2}{3}$
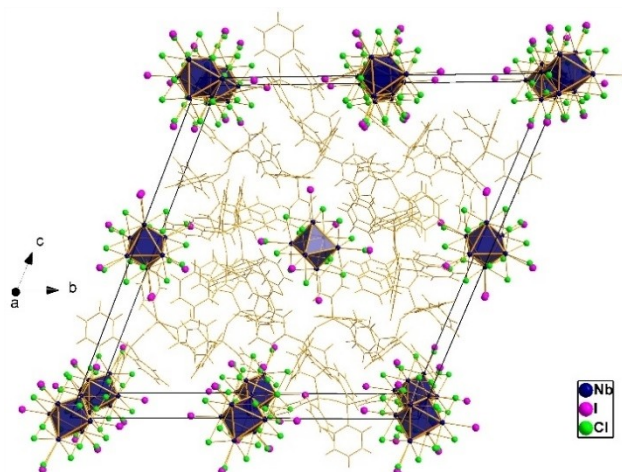
Table 2. Selected atom distances (Å) of the title compounds **1–4**.

	Range	average
$(Ph_4P)_3[Nb_6Cl_{12}I_6]$ (**1**)		
Nb–Nb	2.9771(7)–2.9897(7)	2.9831
Nb–Cl^i	2.426(1)–2.446(1)	2.435
Nb–I^a	2.9080(6)–2.9385(6)	2.9230
$(Ph_4P)_2[Nb_6Cl_{12}I_6]\cdot 4\,CH_2Cl_2$ (**2**)		
Nb–Nb	3.0268(3)–3.0308(3)	3.0293
Nb–Cl^i	2.4228(4)–2.4301(4)	2.4263
Nb–I^a	2.8652(5)–2.8762(5)	2.8708
$(PPN)_3[Nb_6Cl^i_{12}\,I^a_{5.047(9)}Cl^a_{0.953}]$ (**3**)		
Nb–Nb	2.9659(7)–2.9900(7)	2.9798
Nb–Cl^i	2.418(1)–2.451(1)	2.433
Nb–I^a	2.91(1)–2.978(4)	2.932
Nb–Cl^a	2.567(4)–2.567(5)	2.567
$(PPN)_2[Nb_6Cl_{12}I_6]\,2\,CH_2Cl_2$ (**4**)		
Nb–Nb	3.0087(3)–3.0308(3)	3.0211
Nb–Cl^i	2.4082(5)–2.4242(5)	2.4168
Nb–I^a	2.8613(3)–2.8870(3)	2.8773

Figure 5. View of the arrangement of ions in crystals of **3** in a view of the content of the unit cell along *a*. The cations are shown in a wire-stick representation. The Nb_6 octahedra are shown as dark blue polyhedral.

π-π Interactions are also present between the phenyl rings of the $(PPN)^+$ cation in **4**, which are arranged parallelly and offset with a centre···centre distance of 4.234 Å. Further weak hydrogen bonds of the type C–H···I^a exist between the co-crystallized CH_2Cl_2 molecules and I^a atoms with a D···A distance of 4.229 Å.
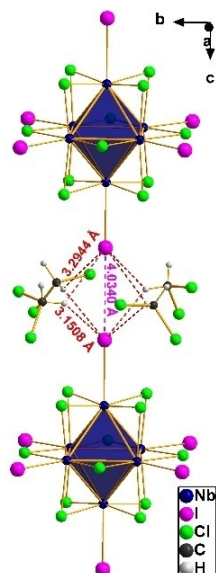
Table 3. Qualitative solubility of **2** in common solvents.

Solvent	Solubility
pentane, toluene	insoluble
ethyl acetate, EtOH, MeOH, dioxane, CHCl$_3$	low soluble
acetone, CH_3CN THF, CH_2Cl_2, DMSO, DMF, pyridine	well soluble

Solubility

The solubility of $(Ph_4P)_2[Nb_6Cl_{12}I_6]\cdot 4CH_2Cl_2$ (**2**) in some common solvents has been determined qualitatively. The results are shown in Table 3.

As expected, the ionic cluster salt **2** is not soluble in non-polar and well soluble in polar solvents. It is interesting to note, that **2**, in contrast to neutral cluster compounds of the type $[Nb_6Cl_{14}L_4]$ with L = organic ligand, is well soluble in the aprotic

ChemistryOpen

Research Article
doi.org/10.1002/open.202200063

Chemistry Europe
European Chemical
Societies Publishing

Figure 6. View of the intermolecular halogen bonding within chains of the cluster units running along the crystallographic *c* direction and hydrogen bonding between the outer iodine atoms and the H atoms of co-crystallized dichloromethane molecules in crystals of **2**.
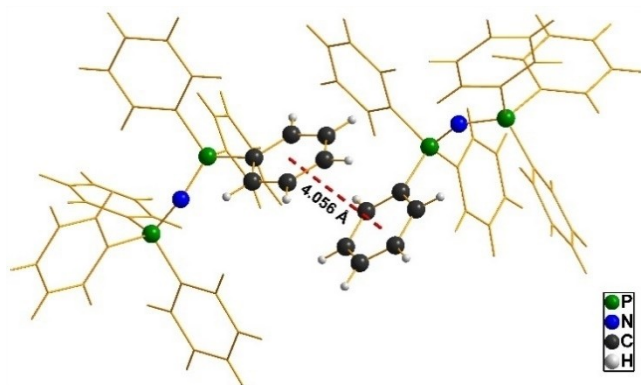

Figure 7. π-π Interactions, marked by a red dashed line, between phenyl rings of neighbouring cations in crystals of **3**.

THF. This might enable the possibility to perform organometallic chemical reactions at the cluster core.

XPS Investigations

The cluster salts described in this article comprise oxidized cluster units with respect to the starting compound. To further characterizes these compounds X-ray photoelectron spectroscopic measurements were done on all four compounds. Figure 8 shows the Nb 3d binding energy spectra of **1**–**4**.

In the binding energy region of Nb 3d, three intensity maxima are visible, which can be de-convoluted into two doublets, of which one of each overlaps with one of the other, such that they together form the middle peak in the spectra. They are related to the two different bonding conditions of the inner and outer halides. Comparing the spectra of the 14 CBE
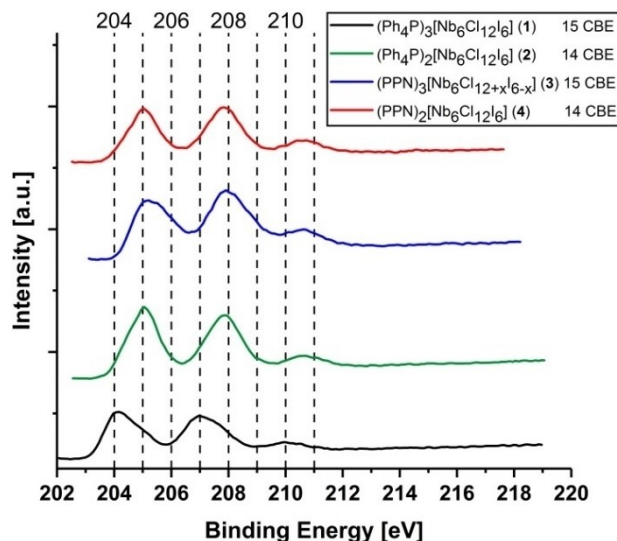
Figure 8. Nb 3d binding energy spectra of **1**–**4**.

with those of the 15 CBE clusters no significant shift of the peak maxima is visible. Whereas the spectra of the two 14 CBE cluster units (**2** and **4**, green and red line in Figure 8) are almost identical, the maxima of **3** (blue line) are slightly shifted even to higher energy, whereas those of **1** (black line) are found at ≈ 1 eV lower energy. This is in accordance with previous reports, which state that variations in the metal oxidation states are not reflected by any significant changes in the metal binding energy, because the charge variations are delocalized over the six metal atoms.[69–70]

Conclusion

An efficient synthetic protocol is presented by which it is possible to prepare $[Nb_6Cl^i_{12}I^a_6]^{n-}$ cluster compounds, which have the outer ligand positions selectively occupied by iodide ligands. In these processes the cluster core is either one- or two-electron ($n=2$ or 3) oxidized. Both structures are characterized by good solubility in various organic solvents. Especially, the good solubility of **2** in THF might allow in future experiments to modify the cluster cores through organometallic chemical reactions.

Experimental Section

General: All chemicals, which were not synthesised as described below, were purchased from commercial suppliers. Because of the moisture and air sensitivity of some compounds all handling is done in carefully dried apparatuses under Schlenk conditions or in an argon filled glove box.

NaCl and niobium powder are dried under high vacuum (10^{-6} mbar) at 600 °C for several hours. (Ph$_4$P)I (TCI, > 98%), Ac$_2$O (VWR, 99%), CH$_2$Cl$_2$ (barrel stock), and (TMS)I (abcr, 97%, stored in a fridge under argon) were used as obtained without further purification.

ChemistryOpen

Research Article
doi.org/10.1002/open.202200063

Chemistry Europe
European Chemical
Societies Publishing

Single-Crystal X-ray Structure Determinations: X-ray diffraction data of single crystals were measured on either a Bruker-Nonius Apex Kappa II diffractometer with fine focus tube, monochromator, Oxford-Cryosystem Cooler and a CCD detector or a Bruker D8 Quest diffractometer with micro focus X-ray tube, Bruker-Kryoflex low temperature Cooler and an Apex-Smart CCD Pixel Array Detector.[71] Mo—Kα radiation, $\lambda = 0.71073$ Å, was used in both cases. Structure solutions and refinements were done with the aid of the Shelx-14 program package.[72–75] All heavy atoms are refined anisotropically. In the final structure refinements, the hydrogen atoms were placed on positions assuming idealized geometry and refined using riding models. In the structure of **3** the outer iodine sites are not full occupied, some clusters have chlorine atoms located more closely at the niobium than the iodine atoms (mixed occupation). These were refined as split sites with the sum of the occupational factors being fixed to unity. Further mixing with hydroxide ions on these sites, accidentally introduced through impurity water molecules, could not be confirmed. Figures of the compounds were prepared with the program DIAMOND, Version 4.6.3.[76]

Deposition Numbers 2143057 (for **1**), 2143059 (for **2**), 2143060 (for **3**), and 2143061 (for **4**) contain the supplementary crystallographic data for this paper. These data are provided free of charge by the joint Cambridge Crystallographic Data Centre and Fachinformationszentrum Karlsruhe href=http://www.ccdc.cam.ac.uk/structures.

NMR Spectroscopy: NMR data were collected with a Bruker AVANCE 250 or a Bruker AVANCE 300 device.

Elemental Analysis: Elemental analyses (C, H, N) were done using a Thermo Quest Flash EA 1112 analyser.

Infrared Spectroscopy: Infrared spectra in the range of 4000–500 cm^{-1} were obtained with a Bruker Alpha FTIR spectrometer. Both are equipped with ATR devices.

Powder X-ray Diffraction: Powder X-ray diffraction was carried out with a Stoe Stadi P powder diffractometer with Cu-Kα1 radiation ($\lambda = 1.5418$ Å) using a Mythen detector. Measurements were carried out in transmission setup. Data collection and handling was performed with the WinXPow program.[77]

XPS Measurements: Measurements were done with a X-ray photo-electron spectroscope (XPS) (ESCALAB 220iXL, Thermo Fisher Scientific). The XPS is equipped with a monochromatic Al Kα source (E = 1486.6 eV). Samples are prepared on a stainless-steel holder with conductive double-sided adhesive carbon tape. The electron binding energies were obtained with charge compensation using a flood electron source and referenced to the C1s core level of carbon at 284.8 eV (C—C and C—H bonds). For quantitative analysis, the peaks were deconvoluted with Gaussian-Lorentzian curves using the software Unifit 2020. The peak areas were normalized by the transmission function of the spectrometer and the element-specific sensitivity factor, published by J. H. Scofield in 1976.[78]

Solubility of 2 in Common Solvents: To determine a qualitative degree of solubility of the cluster compound **2**, $(Ph_4P)_2[Nb_6Cl_{12}I_6] \cdot 4CH_2Cl_2$, in some common solvents, 20 mg precisely weighted amounts of **2** were mixed with 1 mL of the appropriate solvent in a sample tube. The tube was sealed and shaken for 60 min. Then, visually three different levels of qualitative solubility were obtained. The cluster compound is well soluble if it is completely dissolved. It is of low solubility, if it is not completely dissolved, but the solution has a brown colour. The compound is not dissolved if the solvent remains colourless.

Syntheses

$NbCl_5$ is either purchased from commercial suppliers or prepared from the elements under inert conditions and sublimed.

$Na_4[Nb_6Cl_{18}]$

$Na_4[Nb_6Cl_{18}]$ is synthesized using a modified version of a literature-known procedure:[61–62] 9.00 g NaCl (154.00 mmol), 11.56 g niobium powder (124.43 mmol, Chempur 99.9%, <65 micron), and 29.10 g $NbCl_5$ (107.71 mmol) are finely ground in a glovebox using a mortar and the homogenized reactant mixture is divided and filled in two thick-walled fused silica ampoules (length: 25 cm, outer diameter: 1 cm, wall thickness: 2 mm). The filled ampoules are evacuated under high vacuum (10^{-6} mbar) and closed shut by flame. They are heated in a tube furnace from room temperature (RT) to 800 °C within two days, hold at 800 °C for two days and then slowly cooled down to RT within further two days. The yield and purity of the black crystalline product is checked by powder X-ray diffraction.

$[Nb_6Cl_{12}I_2(H_2O)_4] \cdot 4H_2O$[79]

Using a mortar and pestle, the $Na_4[Nb_6Cl_{18}]$ is finely ground and dissolved in 4.0 L of degassed water and stirring at room temperature over a period of two days under low-oxygen conditions. The dark green solution is filtered and concentrated to about half of the volume by a rotary evaporator. To this solution, 500 g of hydroiodic acid (57%, 2228.11 mmol HI, Alfa Aesar) and 1000 g of NaI (6671.56 mmol) are added slowly and stirred for one more day to complete precipitation. A black precipitate is obtained, which is filtered off through a G4 frit and washed several times with cold acetone. The black-green crystalline material is dried at 60 °C for several hours. An amount of 43.20 g (31.30 mmol, yield: 87%) of $[Nb_6Cl_{12}I_2(H_2O)_4] \cdot 4H_2O$ is obtained. The product is characterized by X-ray powder diffraction. A powder diffractogram of $[Nb_6Cl_{12}I_2(H_2O)_4] \cdot 4H_2O$ which was precipitated exclusively using hydroiodic acid has served as a basis for comparison. Both diffractograms are in good agreement. The exclusive use of hydroiodic acid for precipitation is very expensive compared to synthesis using also NaI, since very large amounts are required. The synthesis as described by Schäfer et al.[80] with methanol as solvent is not used, because, even after multiple washing and drying at elevated temperatures in high vacuum, methanol is still detectable in the NMR spectrum.

μ-Nitrido-bis(triphenylphosphan)-iodide (PPN)I[81]

6.5 g (11.32 mmol) (PPN)Cl (97%, Alfa Aesar) are placed in a 100 mL screw-top flask together with 50.0 g (301.20 mmol) KI and 80 mL (4.44 mol) H_2O and stirred at 60 °C for two days. After cooling, the slightly yellowish precipitate is washed several times with water and dried at 60 °C under high vacuum (10^{-6} mbar) for 8 h. Yield: 7.2 g (96%)

$(Ph_4P)_3[Nb_6Cl_{12}I_6]$ (1)

Amounts of 200 mg (144.8 µmol) $[Nb_6Cl_{12}I_2(H_2O)_4] \cdot 4H_2O$, 400 mg (857.8 µmol) $(Ph_4P)I$, and 8.0 mL (84.63 mmol) Ac_2O are filled in a 8.5 mL sample tube and heated for 10 d at 60 °C in a sand bath. Large black single crystals form in the light-coloured sediment, which has separated from the dark solution. For EA, IR, and NMR analyses, the crystals are manually separated from the sediment, washed three times with Ac_2O, CH_2Cl_2, and Et_2O, ground and dried at 60 °C for at least five hours in high vacuum.

ChemistryOpen

Research Article
doi.org/10.1002/open.202200063

**Chemistry
Europe**
European Chemical
Societies Publishing

Yield: 288 mg (72%)

IR: (300 K, ATR, cm^{-1}): 449 (m), 521 (vs), 614 (m), 684 (s), 719 (s), 748 (m), 842 (w), 880 (w), 923 (w), 993 (m), 1026 (w), 1104 (m), 1160 (w), 1185 (w), 1313 (w), 1335 (w), 1434 (m), 1480 (w), 1582 (w).

Elemental Analysis: calcd. (%) for $C_{72}H_{60}Cl_{12}I_6Nb_6P_3$, $M = 2762.46$ g·mol^{-1}: C 31.31, H 2.19; found C 31.64, H 2.30.

^{1}H NMR: ([D$_6$]DMSO), 250 MHz, 300 K, ppm): $\delta = 7.68–7.87$ (m, 48H, H^{ortho}Ph + H^{metha}Ph), 7.92–8.02 (m, 12H, H^{para}Ph).

^{13}C{^{1}H} NMR: ([D$_6$]DMSO, 250 MHz, 300 K, ppm): $\delta = 117.67$ (s, C^{ipso}Ph), 130.43 (s, C^{metha}Ph), 134.52 (s, C^{ortho}Ph), 135.34 (s, C^{para}Ph).

$(Ph_4P)_2[Nb_6Cl_{12}I_6]\cdot4\ CH_2Cl_2$ (2)

Weighted amounts of 1000 mg (724.4 µmol) $[Nb_6Cl_{12}I_2(H_2O)_4]\cdot4H_2O$ and 1000 mg (2.14 mmol) (Ph$_4$P)I are stirred for one hour in a mixture of 20.0 mL (0.31 mol) CH$_2$Cl$_2$, 20.0 mL (0.21 mol) Ac$_2$O, and 5.0 mL (36.73 mmol) (TMS)I in a 50 mL sample tube. Afterwards the mixture is heated at 40 °C in a sand bath for four days. Large black single crystals have separated along with some amorphous sediment from the dark solution. For EA, IR and NMR analyses crystals are separated manually and washed four times with Et$_2$O, ground and dried for at least five hours at 60 °C in high vacuum (10^{-6} mbar).

Yield: 1580 mg (90%)

IR: (300 K, ATR, cm^{-1}): 435 (m), 451 (m), 523 (vs), 616 (m), 684 (s), 719 (s), 750 (m), 840 (w), 923 (w), 995 (m), 1026 (w), 1104 (s), 1162 (w), 1183 (w), 1263 (w), 1311 (w), 1335 (w), 1434 (m), 1480 (w), 1583 (w).

Elemental Analysis: calcd. (%) for $C_{48}H_{40}Cl_{12}I_6Nb_6P_2$, $M = 2423.07$ g·mol^{-1}: C 23.79, H 1.66; found C 23.73, H 1.74.

^{1}H NMR: ([D$_6$]DMSO), 250 MHz, 300 K, ppm): $\delta = 7.68–7.87$ (m, 48H, H^{ortho}Ph + H^{metha}Ph), 7.92–8.01 (m, 12H, H^{para}Ph).

^{13}C{^{1}H} NMR: ([D$_6$]DMSO, 250 MHz, 300 K, ppm): $\delta = 117.67$ (s, C^{ipso}Ph), 130.43 (s, C^{metha}Ph), 134.52 (s, C^{ortho}Ph), 135.32 (s, C^{para}Ph).

$(PPN)_3[Nb_6Cl^i_{12}I^a_{5.047(9)}Cl^a_{0.953}]$ (3)

Amounts of 200 mg (144.8 µmol) $[Nb_6Cl_{12}I_2(H_2O)_4]\cdot4H_2O$ and 400 mg (601.07 mmol) (PPN)I are placed in 8.5 mL sample tube and 8 mL (84.63 mmol) Ac$_2$O are added. The tube is heated for 1 week at 60 °C in a sand bath. Large black tiles crystallize within some light-coloured sediment from the dark solution. For EA, IR, and NMR measurements, the crystals are washed three times with Ac$_2$O and Et$_2$O, ground, and dried at 60 °C for at least five hours in high vacuum (10^{-6} mbar). For the generation of single crystals, the crude product is dissolved in a small amount of CH$_2$Cl$_2$ and the solution is allowed to stand motionless at room temperature for several days.

Yield: 322 mg (68%)

IR: (300 K, ATR, cm^{-1}): 441 (m), 499 (s), 530 (vs), 544 (m), 616 (m), 688 (s), 721 (s), 744 (m), 791 (w), 849 (w), 880 (w), 997 (w), 1024 (w), 1072 (w), 1113 (m), 1162 (w), 1183 (w), 1265 (m), 1284 (m), 1298 (m), 1393 (w), 1434 (m), 1482 (w), 1517 (w), 1587 (w), 1667 (vw).

Elemental Analysis: calcd. (%) for $C_{108}H_{90}N_3P_6Nb_6Cl_{12.953}I_{5.047(9)}$, $M = 3272.91$ g·mol^{-1}: C 39.65, H 2.77; found C 40.22, H 2.74.

^{1}H NMR: ([D$_6$]DMSO), 300 MHz, 300 K, ppm): $\delta = 7.50–7.65$ (m, 72 H, H^{ortho}Ph + H^{metha}Ph), 7.66–7.76 (m, 18 H, H^{para}Ph).

^{13}C{^{1}H} NMR: ([D$_6$]DMSO, 300 MHz, 300 K, ppm): $\delta = 126.78$ (d, JCP = 109 Hz, C^{ipso}Ph), 129.32–129.67 (m, C^{metha}Ph), 131.77–132.15 (m, C^{ortho}Ph), 133.64 (s, C^{para}Ph).

$(PPN)_2[Nb_6Cl_{12}I_6]\cdot2\ CH_2Cl_2$ (4)

A 50 mL sample tube is filled with 1000 mg (724.4 µmol) $[Nb_6Cl_{12}I_2(H_2O)_4]\cdot4H_2O$, 1000 mg (1.50 mmol) (PPN)I, 20.0 mL (0.31 mol) CH$_2$Cl$_2$, 20.0 mL (0.21 mol) Ac$_2$O, and 5.0 mL (36.73 mmol) (TMS)I. It is heated in a sand bath at 40 °C for one week. Large black single crystals form along with small amounts of amorphous sediment from the dark coloured solution. For EA, IR and NMR measurements, the crystals are washed four times with Et$_2$O, ground and dried for at least five hours at 60 °C in high vacuum (10^{-6} mbar).

Yield: 2398 mg (85%)

IR: (300 K, ATR, cm^{-1}): 429 (m), 453 (m), 499 (vs), 530 (vs), 544 (s), 616 (m), 664 (m), 686 (vs), 719 (s), 742 (m), 791 (w), 849 (w), 929 (w), 973 (m), 995 (m), 1024 (m), 1069 (m), 1111 (s), 1158 (m), 1183 (m), 1259 (s), 1294 (m), 1309 (w), 1434 (m), 1482 (w), 1574 (w), 1587 (w).

Elemental Analysis: calcd. (%) for $C_{72}H_{60}N_2P_4Nb_6Cl_{12}I_6$, $M = 2821.45$ g·mol^{-1}: C 30.65, H 2.14; found C 30.47, H 2.20.

^{1}H NMR: ([D$_6$]DMSO), 250 MHz, 300 K, ppm): $\delta = 7.49–7.65$ (m, 48 H, H^{ortho}Ph + H^{metha}Ph), 7.66–7.76 (m, 12 H, H^{para}Ph).

^{13}C{^{1}H} NMR: ([D$_6$]DMSO, 250 MHz, 300 K, ppm): $\delta = 126.79$ (d, JCP = 108 Hz, C^{ipso}Ph), 129.28–129.66 (m, C^{metha}Ph), 131.74-132.14 (m, C^{ortho}Ph), 133.64 (s, C^{para}Ph).

Acknowledgement

Conflict of Interest

The authors declare no conflict of interest.

Data Availability Statement

The X-ray diffraction data that support the findings of this study is deposited and available from the CCDC. All other data is retrievable from the authors.

[1] P. Braunstein, L. A. Oro, P. R. Raithby (Eds.), *Metal Clusters in Chemistry*, Wiley-VCH, Weinheim/Germany, **1999**.

[2] M. H. Chisholm (Eds.), *Early Transition Metal Clusters with π-Donor Ligands*, Wiley-VCH, Weinheim, **1995**.

[3] J. D. Corbett, *Dalton Trans.* **1996**, 575–587.

[4] J. D. Corbett, *Inorg. Chem.* **2000**, *39*, 5178–5191.

[5] F. A. Cotton, T. E. Haas, *Inorg. Chem.* **1964**, *3*, 10–17.

[6] S. Dehnen (Ed.), *Clusters – Contemporary Insight in Structure and Bonding*, Springer, Cham, **2017**.

[7] J. P. Fackler Jr. (Ed.), *Metal-Metal Bonds and Clusters in Chemistry and Catalysis*, Springer, New York, **1990**.

[8] T. Fehlner, J. F. Halet, J. Y. Saillard (Eds.), *Molecular Clusters: A Bridge to Solid-State Chemistry*, Cambridge University Press, **2007**.

[9] T. Hughbanks, *J. Alloys Compd.* **1995**, *229*, 40–53.

[10] G. Meyer, D. Naumann, L. Wesemann (Eds.), *Inorganic Chemistry in Focus III*, Wiley-VCH, Weinheim, **2006**.

[11] D. M. P. Mingos, D. J. Wales (Eds.), *Introduction to Cluster Chemistry*, Prentice Hall, Englewood Cliffs NJ, **1990**.

[12] E. L. Muetterties, T. N. Rhodin, E. Band, C. F. Brucker, W. R. Pretzer, *Chem. Rev.* **1979**, *79*, 91–137.

[13] E. Parthé (Ed.), *Modern Perspectives in Inorganic Crystal Chemistry*, Kluwer Academic Publishers, **1992**.

[14] H. W. Roesky (Ed.), *Rings, clusters, and polymers of main group and transition elements*, Elsevier B. V., Amsterdam, **1989**.

[15] G. Schmid (Ed.), *Clusters and Colloids: From Theory to Application*, VCH, Weinheim, Germany, **1994**.

[16] D. F. Shriver, H. D. Kaesz, R. D. Adams (Eds.), *The Chemistry Of Metal Cluster Complexes*, VCH, Weinheim, Germany, **1990**.

[17] A. Simon, *Angew. Chem. Int. Ed.* **1981**, *20*, 1–22; *Angew. Chem.* **1981**, *93*, 23–44.

[18] A. Simon, *Angew. Chem. Int. Ed.* **1988**, *27*, 159–183; *Angew. Chem.* **1988**, *100*, 163–188.

[19] A. Simon, in *Clusters and Colloids* (Ed.: G. Schmid), VCH, Weinheim, Germany, **1994**, pp. 373–458.

[20] A. Simon, *Pure Appl. Chem.* **1995**, *67*, 311–312.

[21] A. Simon, *Phil. Trans.* **2010**, *A-368*, 1285–1299.

[22] J. D. Corbett, in *Modern Perspectives in Inorganic Crystal Chemistry* (Ed.: E. Parthé), Kluwer Academic Publ., Norwell, MA/USA, **1992**, pp. 27–56.

[23] T. G. Gray, *Coord. Chem. Rev.* **2003**, *243*, 213–235.

[24] J.-F. Halet (Ed.), *Ligated Transition Metal Clusters in Solid-state Chemistry*, Springer, Cham, Switzerland, **2019**.

[25] C. Perrin, *J. Alloys Compd.* **1997**, *262–263*, 10–21.

[26] N. Prokopuk, D. F. Shriver, *Adv. Inorg. Chem.* **1998**, *46*, 1–49.

[27] C. Janiak, H.-J. Meyer, D. Gudat, P. Kurz (Eds.), *Moderne Anorganische Chemie*, De Gruyter, **2018**.

[28] H. Schäfer, H.-G. v. Schnering, *Angew. Chem. Int. Ed.* **1964**, *76*, 833–849.

[29] T. Hughbanks, *Prog. Solid State Chem.* **1989**, *19*, 329–372.

[30] P. Lemoine, J.-F. Halet, S. Cordier, in *Ligated Transition Metal Clusters in Solid-state Chemistry: The legacy of Marcel Sergent*, vol. 180 ed. (Ed.: J.-F. Halet), Springer International Publishing, Cham, **2019**, pp. 143–190.

[31] Z. Lin, I. D. Williams, *Polyhedron* **1996**, *15*, 3277–3287.

[32] L. R. Bateman, J. F. Blount, L. F. Dahl, *J. Am. Chem. Soc.* **1966**, *88*, 1082–1084.

[33] J. D. Corbett, H. Imoto, *Inorg. Chem.* **1980**, *19*, 1241–1245.

[34] A. N. Fitch, S. A. Barrett, B. E. F. Fender, A. Simon, *Dalton Trans.* **1984**, 501.

[35] H. J. Meyer, J. D. Corbett, *Inorg. Chem.* **1991**, *30*, 963–967.

[36] A. Simon, J. J. Finley, H. Nohl, E. E. Vogel, H. Imoto, R. E. Camley, V. Zevin, O. K. Andersen, *Phys. Rev. B* **1981**, *46*, 1472–1475.

[37] A. Simon, H. Imoto, *Inorg. Chem.* **1982**, *21*, 308–319.

[38] A. Simon, F. Stollmaier, *Inorg. Chem.* **1985**, *24*, 168–171.

[39] A. Simon, H.-G. von Schnering, H. Schäfer, *Z. Anorg. Allg. Chem.* **1967**, *355*, 295–310.

[40] F. Schröder, M. Köckerling, *Z. Anorg. Allg. Chem.* **2022**, *648*, e202100295.

[41] M. V. Shamshurin, M. A. Mikhaylov, T. Sukhikh, E. Benassi, A. R. Tarkova, A. A. Prokhorikhin, E. I. Kretov, M. A. Shestopalov, P. A. Abramov, M. N. Sokolov, *Inorg. Chem.* **2019**, *58*, 9028–9035.

[42] J. König, I. Dartsch, E. Sperlich, E. Guillamón, R. Llusar, M. Köckerling, *Z. Anorg. Allg. Chem.* **2020**, *646*, 1531–1538.

[43] J. König, I. Dartsch, A. Topp, E. Guillamón, R. Llusar, M. Köckerling, *Z. Anorg. Allg. Chem.* **2016**, *642*, 572–578.

[44] J. König, M. Köckerling, *Chem. Eur. J.* **2019**, *25*, 13905–13910.

[45] J. König, M. Köckerling, *Z. Anorg. Allg. Chem.* **2020**, *646*, 1212–1217.

[46] E. Sperlich, M. Köckerling, *Z. Naturforsch. B* **2019**, *74*, 751–755.

[47] E. Sperlich, M. Köckerling, *Z. Naturforsch. B* **2020**, *75*, 173–181.

[48] E. Sperlich, M. Köckerling, *Inorg. Chem.* **2022**, *61*, 2409–2420.

[49] E. Sperlich, J. König, D. H. Weiß, F. Schröder, M. Köckerling, *Z. Anorg. Allg. Chem.* **2019**, *645*, 233–241.

[50] D. H. Weiß, F. Schröder, M. Köckerling, *Z. Anorg. Allg. Chem.* **2017**, *643*, 345–351.

[51] F. Ogliaro, S. Cordier, J.-F. Halet, C. Perrin, J.-Y. Saillard, M. Sergent, *Inorg. Chem.* **1998**, *37*, 6199–6207.

[52] A. Flemming, M. Köckerling, *Z. Anorg. Allg. Chem.* **2008**, *634*, 2309–2315.

[53] S. Ihmaine, C. Perrin, O. Pena, M. Sergent, *J. Less-Common Met.* **1988**, *137*, 323–332.

[54] F. W. Koknat, R. E. McCarley, *Inorg. Chem.* **1974**, *13*, 295–300.

[55] A. Penicaud, P. Batail, C. Coulon, E. Canadell, C. Perrin, *Chem. Mater.* **1990**, *2*, 123–132.

[56] A. Penicaud, P. Batail, P. Davidson, A. M. Levelut, C. Coulon, C. Perrin, *Chem. Mater.* **1990**, *2*, 117–123.

[57] A. Penicaud, P. Batail, C. Perrin, C. Coulon, S. S. P. Parkin, J. B. Torrance, *J. Chem. Soc. Chem. Commun.* **1987**, 330–332.

[58] M. Ströbele, H. J. Meyer, *Z. Naturforsch.* **2001**, *56b*, 1025–1034.

[59] J. D. Corbett, *J. Solid State Chem.* **1981**, *37*, 335–351.

[60] E. Levi, D. Aurbach, O. Isnard, *Acta Crystallogr.* **2013**, *B69*, 426–438.

[61] A. Simon, H.-G. von Schnering, H. Schäfer, *Z. Anorg. Allg. Chem.* **1968**, *361*, 235–248.

[62] A. Simon, H. G. von Schnering, H. Schäfer, *Z. Naturforsch. B* **1968**, *361*, 235–248.

[63] R. Bishop, *CrystEngComm* **2015**, *17*, 7448–7460.

[64] A. Bondi, *J. Phys. Chem.* **1964**, *68*, 441–451.

[65] G. Cavallo, P. Metrangolo, R. Milani, T. Pilati, A. Priimagi, G. Resnati, G. Terraneo, *Chem. Rev.* **2016**, *116*, 2478–2601.

[66] P. Metrangolo, F. Meyer, T. Pilati, G. Resnati, G. Terraneo, *Angew. Chem. Int. Ed.* **2008**, *120*, 6206–6220.

[67] C. A. Hunter, J. K. M. Sanders, *J. Am. Chem. Soc.* **1990**, *112*, 5525–5534.

[68] C. Janiak, *Dalton Trans.* **2000**, 3885–3896.

[69] S. A. Best, R. A. Walton, *Inorg. Chem.* **1979**, *18*, 484–488.

[70] R. A. Walton, D. D. Klendworth, *Inorg. Chem.* **1981**, *20*, 1151–1155.

[71] Apex3, Saint, Sadabs, *Sadabs, Software for the CCD Detector System*, Bruker-Nonius Inc., Madison, WI, USA, **2017**.

[72] G. M. Sheldrick, *Acta Crystallogr.* **1990**, *A46*, 467–473.

[73] G. M. Sheldrick, *Acta Crystallogr.* **2008**, *A64*, 112–122.

[74] G. M. Sheldrick, *Acta Crystallogr.* **2015**, *A71*, 3–8.

[75] G. M. Sheldrick, *Acta Crystallogr.* **2015**, *C71*, 3–8.

[76] DIAMOND, Crystal Impact GbR, Bonn, Germany, **2019**.

[77] WinXPOW, STOE & Cie GmbH, Darmstadt/Germany, **2009**.

[78] J. H. Scofield, *J. Electron Spectrosc. Relat. Phenom.* **1976**, *8*, 129–137.

[79] F. W. Koknat, J. A. Parsons, A. Vongvusharintra, *Inorg. Chem.* **1974**, *13*, 1699–1702.

[80] H. Schäfer, B. Plautz, H. Plautz, *Z. Anorg. Allg. Chem.* **1972**, *392*, 10–22.

[81] A. Martinsen, J. Songstad, *Acta Chem. Scand.* **1977**, *31a*, 645–650.